1st Cirp Conference on Composite Materials Parts Manufacturing, cirp-ccmpm2017

Investigation of a new approach for additively manufactured continuous fiber-reinforced polymers

M.Sc. Florian Baumann[a],*, M.Sc. Julian Scholz[b], Prof. Dr.-Ing. Jürgen Fleischer[a]

[a] KIT Karlsruhe Institute of Technology – wbk Institute of Production Science, Kaiserstraße 12, 76131 Karlsruhe, Germany
[b] Apium Additive Technologies GmbH, Willy-Andreas-Allee 19, 76131 Karlsruhe, Germany

* Corresponding author. Tel.: +49-721-608-44012; fax: +49-721-608-45005. E-mail address: florian.baumann@kit.edu

Abstract

First additive manufacturing processes (AM) for the production of fiber reinforced plastics (FRP) have been developed, which use Fused Layer Modelling (FLM) processes by implementing the fibers into the matrix material prior to extruding or within the nozzle. A method for implementing the fibers outside of the printing nozzle and outside of the thermoplastic filaments directly into the part while it is being manufactured has not yet been analyzed properly. This study shows the gain in tensile strength and Young's modulus for different implementation methods of glass and carbon fibers on the building platform.

1. Introduction

A relatively new field of additive manufacturing technologies (AMT) is the production of fiber reinforced polymers (FRP). Some processes use stereolithography (SLA) [1, 2] for additively manufacturing FRPs, but most use fused layer Modeling (FLM) sometimes also named fused deposition modeling (FDM) or fused filament fabrication (FFF) [3–8]. Thanks to companies like Arevo Labs, everybody with a cheap FLM printer can print FRP parts due to their short fiber reinforced polymer filaments [9].

The mechanical properties of FRPs, especially tensile strength and Young's modulus, increase with the length of the fibers [10]. So in order to additively manufacture parts for high performance use, continuous fiber-reinforcements need to be used.

2. Additive manufacturing of continuous fiber reinforced polymers

As shown previously, fiber reinforcements are most often used in FLM processes. FLM processes usually use one or more nozzles to locally extrude molten thermoplastic in order to additively manufacture a part [11]. Since the extrusion process itself generates a 2-dimensional string of thermoplastic, the fiber rovings can be implemented very easily by placing them directly into the extruded material.

In general, there are three different ways to implement continuous fibers into a printjob in FLM processes [4]:

- The fibers can be placed into the printing filaments prior to the nozzle, which usually implies the need for a prepreg material.
- In addition, the fibers can be implemented into the matrix material inside the nozzle. This way, a wide selection of fiber-matrix-combinations can be achieved.
- The third method for implementing the continuous fibers into the matrix material is after the matrix material passed the nozzle while the part is being manufactured.

Fig. 1 shows the aforementioned points from left to right. Grey areas are the nozzles, green strings are the extruded thermoplastic and the black strings are fibers.
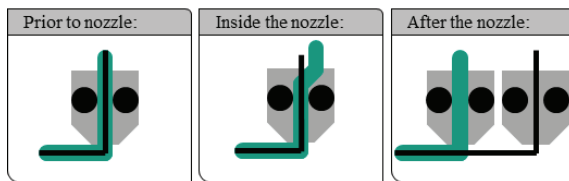
Fig. 1: Methods of fiber implementation based on [12]

Implementing the fibers prior to the nozzle is done by Markforged for use in their MarkOne, MarkTwo and MarkX printers, the only commercially available printers which can manufacture continuous FRP [6]. Research to a similar process is being done in Dresden [8].

Research about the implementation of continuous fibers inside the nozzle is being done by [4, 5, 7]. General disadvantages of this implementation method are the more difficult process control due to the fiber infiltration parallel to printing and the handling of the fibers [4].

Implementing the fibers after the nozzle directly into the printjob is done by Mori et al. with carbon fibers and acrylonitrile butadiene styrene (ABS). Their research shows, that the carbon fibers were entirely pulled out of a ruptured tensile test specimen and the fibers affected the resulting tensile strength only a little. With an additional thermal bonding the test specimen reached about double of the tensile strength of unreinforced specimens [5]. The shown results should be perceived with care. Since the tensile strength without fibers was only at 11MPa, about a quarter of common values of ABS, the quality of the FLM process in this case is more than questionable.

When the 3D-printer has only one nozzle, both methods of fiber implementation "prior to nozzle" and "inside the nozzle" result in the whole print job being made out of FRP. This may be useful in some cases, but the more efficient and economical way of fiber implementation is by placing the fibers only where they are absolutely needed. Only method 3 "after the nozzle" allows the local addition of fibers, so it gets addressed by the research shown in this manuscript.

3. Experimental Design

To integrate continuous fibers in the additive manufacturing process following method 3 "after the nozzle", three different approaches are being developed and evaluated:

- Concept 1: Direct overprinting of the fiber rovings
- Concept 2: Insertion of the fiber rovings through a hypodermic needle
- Concept 3:Using a solvent

Following fibers are chosen to manufacture the test specimens:

- Carbon fibers: Torayca T300 1K
- Glass fibers: 3B Advantex SE 1200 300 tex

As matrix material the ABS Cycolac CTR52 is being chosen. Five Tensile test specimens similar to specimens of DIN EN ISO 527 are printed for each concept and each fiber type using the additive manufacturing system Arburg freeformer. Every test specimen is printed with a layer thickness of 0.265mm and consists of 14 layers. The infill parameters are chosen in a way that the specimens have a theoretical porosity of 0%. The fibers are being inserted according to each approach between layers seven and eight in order to produce a symmetric specimen with reduced warping.

3.1. Experimental setup

Since the fiber rovings are placed between the seventh and eighth layer of each specimen, the printing model needs to be divided into a bottom half and a top half. The bottom half has to be taken out of the 3D-printer's building chamber to integrate the fibers. When it is put back into the printing chamber, the correct positioning and fixing is necessary. Therefore, the standard ISO 527 test specimens have to be edited by adding six small wings on the specimen's side, on which small struts are placed to hold the specimens in place, also see Fig. 2.
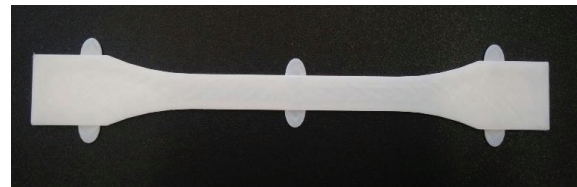
Fig. 2: Bottom half of test specimen

The positioning is ensured by putting the bottom half between six pins. The procedure for 3D-printing a FRP specimen is as follows:

- Print bottom half
- Insert fiber rovings, see chapters 3.2 to 3.4
- Position bottom half on the building platform
- Fix bottom half with small struts
- Heat building chamber to 80°C
- Print top half

Fig. 3 shows the positioned and fixed specimen including the fibers on top of the building platform.

Fig. 3: Building platform with specimen

3.2. Concept 1: Direct overprinting

The fiber rovings are laid down on the surface of the seventh layer as shown in Fig. 3. They are fixed in place on the sides of the building platform. The loose fibers get embedded in the part by printing on top of them. No other means of fixture/adhesion is used.

3.3. Concept 2: Hypodermic needle

In this approach, the fiber roving is guided through a heated hypodermic needle as used in medicine and pressed on the surface of the printed layer. The needle is systematically dragged over the surface of the printed layer while the fibers are deposited on its trail. This set-up is operated with the temperature of the needle being higher than the melting temperature of the matrix material. Therefore, the portion of material around the contact surface of the needle is molten. The fibers discharged from the lower end of the needle are pressed directly in the liquid phase of the matrix causing the fibers to adhere to the specimen. A cross section of the needle implementing fibers in the specimen is shown in Fig. 4.

Fig. 4: Implementing fibers with a heated hypodermic needle

After implementing the fiber rovings in the specimen, it is put on the building platform shown in Fig. 3 and the process continues according to chapter 3.1.

3.4. Concept 3: Solvents

This approach of implementing the fiber rovings involves the application of a thin film of solvent on the surface of the printed layer, thus forming a solution of solvent and matrix material. Since ABS is used for the matrix material, acetone is chosen as solvent. After applying the acetone to the top of the specimen, the fibers are laid down in the resulting solution on the material surface. Once all acetone is vaporized the fibers remain wetted with a thin coat of ABS material and adhere to the specimen. Fig. 5 shows fibers put on top of the specimen and adhering by formerly dissolved matrix material.
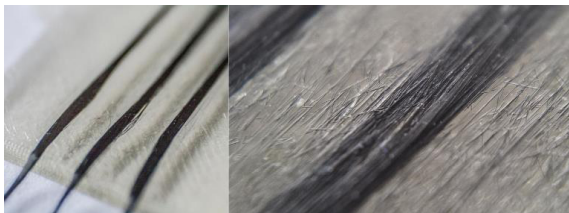
Fig. 5: Fiber adhesion trough acetone

According to Concept 2, the test specimens are put on the building platform shown Fig. 3 and the process continues according to chapter 3.1 after implementing the fiber rovings.

Opposed to Concept 1, where the fiber rovings need to be fixed to the building platform as shown in Fig. 3, Concepts 2 and 3 result in fiber rovings adhering to the bottom half of the specimen. Those specimen look very much alike and are shown exemplary for Concept 2 in the following Fig. 6.

Fig. 6: Bottom half of the test specimens with implemented glass fibers (top) and carbon fibers (bottom)

The following Table 1 shows an overview over all specimens. For each series five different specimens are manufactured. The specimen series R is the reference, it is manufactured according to chapter 3.1, just without any fiber implementation.

In order to achieve the maximal performance, as many rovings as possible should be implemented in the specimens. However, it also should be considered, that by implementing too many fibers in one layer, the top half of a specimen might not be entirely bonded to the bottom half. Therefore, the specimens C1-C3 have three carbon fiber rovings with each 1.000 filaments (1K roving); the specimens G1-G3 have two glass fiber rovings with each 300 tex.

For a better comparison between carbon fibers and glass fibers, the filament count of the carbon fiber roving is converted into tex (1.000 filaments ≙ 66tex).

Table 1: Overview

Specimen name	description	Fiber implementation approach
R	Reference	-
C1	3x66 tex CF	Concept 1: direct overprint
C2	3x66 tex CF	Concept 2: hypodermic needle
C3	3x66 tex CF	Concept 3: solvent
G1	2x300 tex GF	Concept 1: direct overprint
G2	2x300 tex GF	Concept 2: hypodermic needle
G3	2x300 tex GF	Concept 3: solvent

The fiber volume content (FVC) is calculated using following formulas (1) to (3).

$$\varphi = \frac{V_f}{V_{specimen}} * 100\% \qquad (1)$$

with

$$V_f = \frac{n * y_c * l}{\rho} \qquad (2)$$

$$V_{specimen} = l * w * h \qquad (3)$$

φ ≙ *fiber volume content*
V_f ≙ *fiber volume*
V_m ≙ *matrix volume*
n ≙ *number of fiber rovings*
y_c ≙ *yarn count*
l ≙ *length of specimen*
$ρ$ ≙ *density of fibers*
w, h ≙ *width, height of specimen in breaking area*

Table 2 shows the given values for the specimens.

Table 2: Values needed for calculating the fiber volume content

	Glass (G1-G3)	Carbon (C1-C3)	unit
n	2	3	[-]
tex	$66*10^{-6}$	$300*10^{-6}$	[g/mm]
l		150	[mm]
ρ	$2,62*10^3$	$1,76*10^3$	[g/mm³]
w		10	[mm]
h		3,8	[mm]

This results in a FVC of 0.3% for the C-series and 0.6% for G-series. Since the FVC is very low, the fibers might lower the tensile strength [13]. Only Young's modulus should be taken into account to compare carbon- and glass-fiber specimens.

4. Results

The fully printed tensile test specimens are tested according to DIN EN ISO 27. In favor of a full representation of the results, the tensile strength including the standard deviation for each series is shown in Fig. 7.
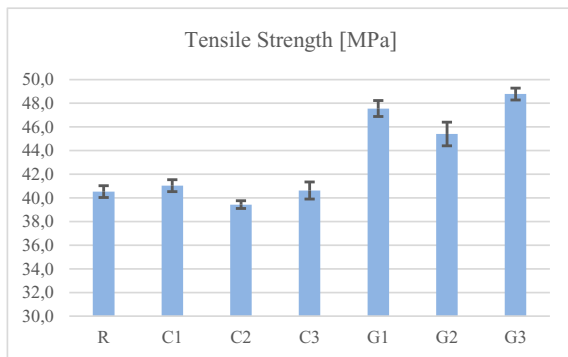
Fig. 7: Tensile strength of 3D-printed FRP

As expected, the tensile strength of all carbon fiber specimens doesn't exceed the reference strength, the FVC is too low for a positive influence on the specimens. Due to the higher FVC of the glass fiber specimens, the tensile strength considerably exceeds the reference specimen and the carbon fiber specimens. According to series C2 a little decrease of strength can be seen in series G2 in comparison to G1 and G3.

A more reliable way of comparing FRPs with a low FVC is the comparison of their Young's moduli. Those, including the standard deviation for each series, are shown in Fig. 8.
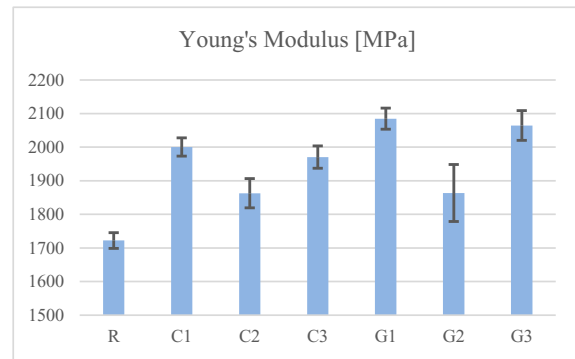
Fig. 8: Young's modulus of 3D-printed FRP

Opposed to the tensile strength, all specimens show a considerable gain in values, since the low FVC has no effect on the stiffness. The glass fiber specimens of series G1 and G3 exceed all carbon fiber specimens due to their higher fiber volume content. Again, series C2 and G2 show considerably lower gain compared to C1 and C3 or G1 and G3 respectively.

For a better comparison between the different fiber types and FVCs, a normalized representation is needed instead of the absolute values given in Fig. 1. Therefore the "stiffening fulfilment" *e* is being introduced. It compares the actual improvement to the calculated improvement of Young's modulus and is calculated in formulas (4) to (7).

$$e = \frac{e_{actual}}{e_{theoretical}} \qquad (4)$$

with

$$e_{actual} = \left(\frac{E_{Xn}}{E_R} - 1 \right) * 100\% \qquad (5)$$

$$e_{theoretical} = \left(\frac{E_X}{E_R} - 1 \right) * 100\% \qquad (6)$$

E_{Xn} ≙ *measured Young's modulus*
Xn ≙ *C1, C2, C3, G1, G2, G3*
E_R ≙ *measured Young's modulus of reference specimen*
E_X ≙ *calculated Young's modulus*

The theoretical Young's modulus E_X is calculated with following formula (7) [10]:

$$E_X = (\varphi_f * E_f + \varphi_m * E_m) \qquad (7)$$

φ_f ≙ *fiber volume content*
E_f ≙ *fiber Young's modulus*
φ_m ≙ *matrix volume content*
E_m ≙ *matrix Young's modulus*

With formulas (5) to (7) and following Table 3, formula (4) can be calculated.

Table 3: Values needed for calculating the *e* in formula (4)

	Glass (G1-G3)	Carbon (C1-C3)	unit
φ_f	0,6	0,3	%
E_f	82.000	230.000	[MPa]
φ_m	99,4	99,7	%
E_m		1722	[MPa]

The results are listed in Fig. 9. The 0% value is the reference-Young's modulus, 100% is the maximum stiffening which can be achieved with both carbon fibers and glass fibers.
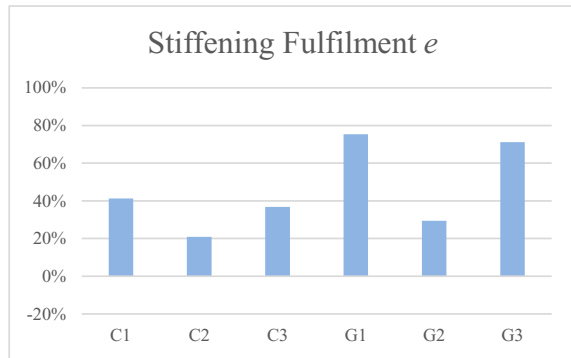
Fig. 9: Actual improvement compared to max. theoretical Improvement (Young's modulus)

Carbon fiber specimens show a stiffening fulfilment of 20 to 40%. Specimens G1 and G3 reach even higher values with 70% to 80%, only series G2 stays at a fulfilment of 30%. Fig. 10 shows the breaking areas of representative specimens for each series.
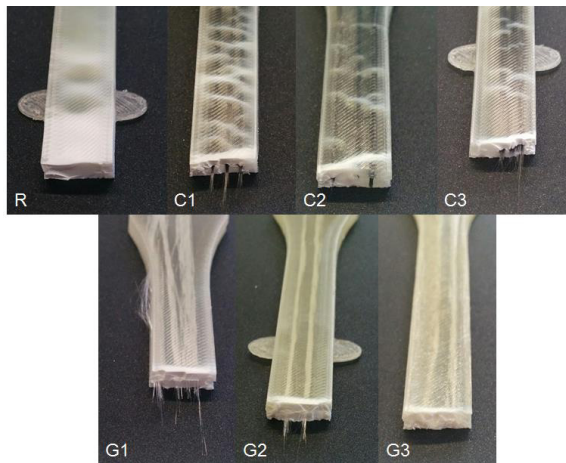
Fig. 10: Examples of test specimens

All specimens show a very clean and smooth polymer-surface of the breaking area.

The previously transparent specimen whitens at the breaking area. Additional some white patterns parallel to the breaking-surface occur with the C-series specimens. Taking a closer look to the breaking area, the occurring fiber pullout decreases from series 1 to 3 for both carbon- and glass fiber specimens, so concept 3 offers the best adhesion between fibers and matrix, followed by concepts 2 and 1.

5. Conclusions

To start with the conclusions, all results are put together in Table 4:

Table 4: Overview of results

	C1	C2	C3	G1	G2	G3
E	++	+	++	++	+	++
e	+	0	+	++	+	++
optical	0	+	0	0	0	++

Since both series, C2 and G2 show lower values in strength (also see Fig. 7) and stiffness, a systematic defect concerning the hypodermic needle seems obvious.

Opposed to series C1 and G1 the fibers are plowed into the bottom half of each specimen. This leads to some impregnation of the fibers by the molten polymer, which is indicated by the fibers adhering to the bottom half. Following, the fiber rovings are embedded in the specimens by a direct print-over as described in chapter 3.3. The added adhesion to the bottom half should in fact result in a higher strength and stiffness than series C1 and G1, since the fibers are not just being infiltrated from above, but also from below. The resulting decrease in strength and stiffness can only be explained by the following points:

- The bottom half gets damaged by plowing the fibers into its surface
- The fibers get damaged by pressing them onto the bottom half's surface

The first point cannot be checked properly by available testing methods. The second point seems more likely, since some crackling of breaking fibers can be heard when embedding them into the bottom half. In addition to the sound, the decrease of series G2 is more significant than the decrease of series C2. Based on the more brittle behavior of glass fibers compared to carbon fibers, more breakage occurs with glass fibers by pressing them into the bottom half. Fig. 4 shows the fibers being bent around the upper edge of the hypodermic needle, at this spot fiber breakage can occur. In conclusion, "concept 2 – hypodermic needle" is not a reasonable choice for embedding the fibers.

Specimens manufactured via concept 1 and concept 3 perform very similar to each other. Comparing the tensile strength, series C1 and C3 perform very similar while G3 outperforms G1 just about 1.5 MPa. Comparing the stiffness of all specimens, C3 and G3 even lose a little compared to C1 and G1 respectively, while the mean values of C3 and G3 are within the standard deviation of the respective concept 1 values.

Since the fibers in concept 3 adhere to the bottom half, an increase of strength and stiffness was expected.

The following points could explain the mediocre performance of the series 3 specimens:

- Acetone weakens the polymer
- Direct overprinting reaches the same level of adhesion between fibers and bottom half by melting the surface of the bottom half through the thermal energy of the top half's first layer

Taking all measured values (strength and stiffness) into account, the glass fiber specimens outperform the carbon fiber specimens. Since the specimens use different fiber volume contents, a more reliant comparison can be taken with the strengthening- and stiffening fulfilment because the theoretical maximum values are taken as a standard value.

In conclusion, the best setup for implementing fibers during additive manufacturing when choosing between the named concepts and glass and carbon fibers, is concept 1 – direct overprint with glass fibers. Since it only fulfilled its theoretical performance by 50% to 80%, there obviously is no 100% adhesion between fibers and matrix. But nevertheless a significant gain in tensile strength by 17% and Young's modulus by 21% can be detected with a fiber volume content of only 0.6%.

Specimens using a carbon fiber volume content of ~6% can be seen in Fig. 11. The corresponding tests have not been completed yet, the complete results will be published at a later point of time.

Fig. 11: Test specimens with ~6% fiber volume content

First results show a Young's modulus of 4400 MPa for direct overprinting and 8400 for implementation by hypodermic needle. On the one hand, this shows, that specimens can also be printed with a higher fiber volume content. On the other hand, opposed to the tests with a low fiber volume content, the implementation by hypodermic needle results in much higher values then direct overprint.

6. Outlook

In the future, more research should be conducted concerning the discrepancy between Young's moduli of concepts 1 and 2 in low and high fiber volume contents. In addition, a different fiber sizing, explicitly manufactured for the use of fibers in ABS should be tested and a thermal bonding like it was conducted by Mori et al. should be implemented.

Considering the process of implementing endless fibers in AM technologies itself, some kind of kinematic will need to be developed to implement the fibers automatically. In addition, the data processing must be updated to enable G-Codes for the manufacturing of FRP.

References

[1] Karalekas, D., Antoniou, K., 2004. Composite rapid prototyping: overcoming the drawback of poor mechanical properties, in *Journal of Materials Processing Technology*, Elsevier, p. 526.
[2] Karalekas, D., 2003. Study of the mechanical properties of nonwoven fibre mat reinforced photopolymers used in rapid prototyping *24*, p. 665.
[3] Zhong, W., Li, F., Zhang, Z., Song, L. *et al.*, 2001. Short fiber reinforced composites for fused deposition modeling *301*, p. 125.
[4] Prüß, H., Vietor, T., 2015. Design for Fiber-Reinforced Additive Manufacturing *137*, p. 111409.
[5] Mori, K.-i., Maeno, T., Nakagawa, Y., 2014. Dieless Forming of Carbon Fibre Reinforced Plastic Parts Using 3D Printer *81*, p. 1595.
[6] MarkForged. MarkForged Homepage: The world's first 3D printer that can print carbon fiber. https://markforged.com/. Accessed 19 September 2016.
[7] Fraunhofer-Institut für Produktionstechnik und Automatisierung IPA, Editor, 2013. *interaktiv - Das Kundenmagazin des Fraunhofer IPA*.
[8] Tanja Kirsten. Leichtbau aus dem 3D-Drucker: Wissenschaftler der TU Dresden machen 3D-Druck mit Hybridgarnen möglich. https://tu-dresden.de/ing/maschinenwesen/ilk/das-institut/news/news_article-2015-10-28-9464270705. Accessed 19 September 2016.
[9] Molitch-Hou, M. Arevo Labs want to See Makers 3D Printing with Carbon Fiber and Carbon Nanotubes. http://3dprintingindustry.com/2014/03/28/arevo-labs-want-see-makers-3d-printing-carbon-fiber-carbon-nanotubes/. Accessed 28 October 2014.
[10] Ehrenstein, G.W., 2006. *Faserverbund-Kunststoffe: Werkstoffe, Verarbeitung, Eigenschaften,* 2nd edn. Hanser, München [u.a.].
[11] Gebhardt, A., Hötter, J.-S., 2016. *Additive manufacturing: 3D printing for prototyping and manufacturing*. Hanser Publishers; Hanser Publications, Munich, Cincinnati.
[12] Prüß, H., Vietor, T., 2015. *Neue Gestaltungsfreiheiten durch 3D-gedruckte Faser-Kunststoff-Verbunde*, Braunschweig.
[13] Haspel, B., 2015. *Werkstoffanalytische Betrachtung der Eigenschaften von mittels neuartiger RTM-Fertigungsprozesse hergestellten glasfaserverstärkten Polymerverbunden*. KIT Scientific Publishing, Karlsruhe.